https://doi.org/10.1016/j.jpowsour.2021.230536

Autothermal reforming of methane over an integrated solid oxide fuel cell reactor for power and syngas co-generation

Dongjie Fan [a], Yi Gao [a], Fangsheng Liu [a], Tao Wei [a], Zhengmao Ye [a,] Yihan Ling [b], Bin Chen [c, *], Yuan Zhang [c], Meng Ni [d], and Dehua Dong [a, *]

[a] School of Materials Science and Engineering, University of Jinan, Jinan, 250022, P.R. China

[b] School of Materials Science and Physics, China University of Mining and Technology, Xuzhou 221116, P. R. China

[c] Shenzhen Key Laboratory of Deep Underground Engineering Sciences and Green Energy, Institute of Deep Earth Sciences and Green Energy, College of Civil and Transportation Engineering, Shenzhen University, Shenzhen 518060, China

[d] Department of Building and Real Estate, Research Institute for Sustainable Urban Development (RISUD) & Research Institute for Smart Energy (RISE), The Hong Kong Polytechnic University, Hung Hom, Kowloon, Hong Kong, China

* Corresponding authors

Bin Chen, Email: chenbin@szu.edu.cn; Tel/Fax numbers: +86-755-2653 6235/+86-755-26733103

Dehua Dong, Email: mse_dongdh@ujn.edu.cn; Tel/Fax numbers: +86-531-89736011/+86-531-87974453

Abstract

Autothermal reforming of methane couples exothermal partial oxidation of methane and endothermal steam or dry reforming of methane to achieve high energy efficiency, which can be operated through solid oxide fuel cells (SOFCs) so that expensive oxygen is not required and safety issue caused by CH_4/O_2 mixture is avoided. In addition, electric power is simultaneously generated. This study has demonstrated the efficient electrochemical autothermal reforming of methane over a SOFC reactor integrated with catalyst beds within anode channel structure. The catalyst bed reformer increases syngas yield by a factor of about 6 owing to the increased methane conversion and syngas selectivity. By numerical assessment, enhanced mass transportation is well validated by high fuel accessibility at the electrode-electrolyte interface benefiting from the integrated catalyst beds. Compared with conventional catalyst layer on anode surface, the catalyst beds are more efficient for conducting methane reforming. After the initial stabilization of cell microstructure, the SOFC reactor has demonstrated stable cell performance and syngas yield during the test for 120 h. The integrated SOFC reactor has demonstrated a promising application in performing catalytic reforming reactions.

Keywords: Autothermal reforming of methane; SOFC reactors; Cogeneration; Numerical assessment

1. Introduction

As fossil fuels are increasingly depleted, efficiently utilizing the fuels has attracted intensive attention [1]. As an important fossil fuel, natural gas with the main component

of methane can be catalytically reformed into syngas (H_2 and CO), which is a feedstock for liquid fuel and chemical production *via* the Fischer-Tropsch process [2, 3]. For example, the synthesized methanol feeds fuel cells to generate power with the higher energy efficiency and the less environmental impact compared with conventional gas-fired power plants [4-6]. Methane is generally reformed into syngas through the following reactions:

Partial oxidation of methane (POM): $CH_4 + 0.5O_2 \rightarrow CO + H_2 \quad \Delta H_1 = -35.6$ kJ/mol

Steam reforming of methane (SRM): $CH_4 + H_2O \rightarrow CO + 3H_2 \quad \Delta H_2 = +206.2$ kJ/mol

Dry reforming of methane (DRM): $CH_4 + CO_2 \rightarrow 2CO + 2H_2 \quad \Delta H_3 = +247.3$ kJ/mol

POM reaction reforms methane with oxygen and generates a favorable H_2/CO ratio of 2 for methanol production [7]. However, oxygen is generated by an expensive cryogenic process, and the exothermal reaction can induce hotspot formation within catalyst beds [8, 9]. SRM and DRM are endothermal reactions, and generate syngas with the H_2/CO ratio of 1 and 3, respectively [10, 11]. Accordingly, autothermal reforming of methane was developed by a combination of POM and SRM or DRM to achieve high energy efficiency and adjustable H_2/CO ratio [12-15].

As shown in Fig. 1, although the autothermal reforming has tackled the thermal issue, it requires expensive oxygen, which also induces safety issue because of the explosive CH_4/O_2 mixture [16]. These two issues can be simultaneously solved by employing solid oxide fuel cells (SOFCs) as an electrochemical reformer [17, 18]. Under the oxygen partial pressure difference between anode and cathode, oxygen is extracted from air on cathode side, and then transported to anode side through

electrolyte in the form of oxygen ion, which participates the autothermal reforming on anode side to generate syngas. The electrochemical autothermal reforming reaction can be presented as:

$$CH_4 + xCO_2 + (1\text{-}x)\ O^{2-} \rightarrow 2H_2 + (1+x)\ CO\ (x = 0\sim1) \quad (1)$$

In addition, electric power is generated during the electrochemical reforming process [19-21].

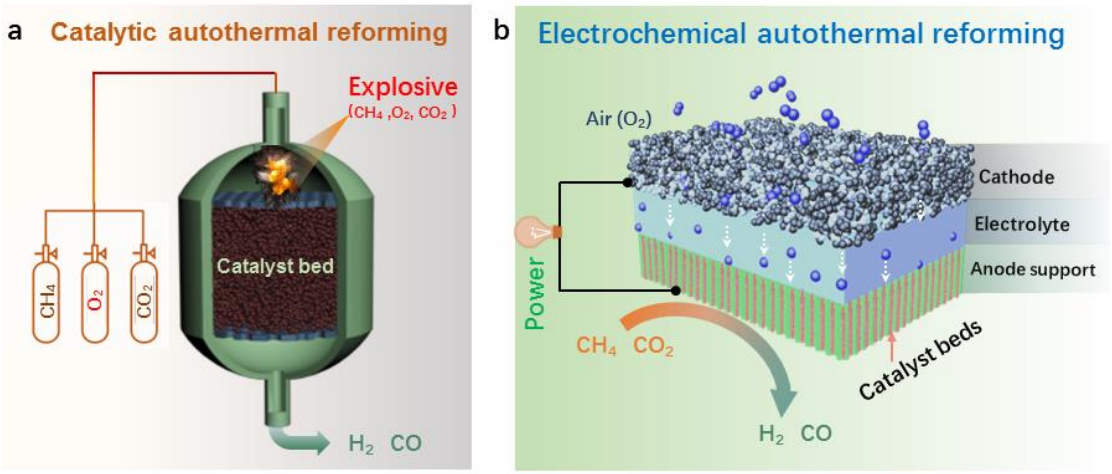

Fig. 1. Schematic comparison of (a) conventional autothermal reforming of methane within catalyst bed reactors and (b) electrochemical autothermal reforming of methane over SOFCs.

Using methane as a fuel for SOFCs has been widely studied. However, it is still challenging to directly use methane for the state-of-the-art Ni-based anodes. The coarse nickel particles of anodes formed during high-temperature sintering show low catalytic activity for the electrochemical oxidation of methane and resistance to carbon deposition [22, 23]. Many attempts have been made to improve the performance of methane-fueled SOFCs. There are generally two strategies: adding reforming agents

and applying reforming catalysts. Reforming agents (e.g. O_2, CO_2 or H_2O) are added with methane in feeding gas to reform methane into syngas, which acts as a fuel for power generation [24, 25]. Thereby, methane is an indirect fuel for SOFCs, and it aims at power generation. Although direct-methane SOFCs have demonstrated the feasibility of power and syngas co-generation. Few studies focus on the performance of syngas generation because the Ni-based anodes show low catalytic activity and syngas selectivity is limited by gas diffusion within porous anodes. The SOFC reactors developed for the electrochemical autothermal reforming in this study focus on syngas generation, though they simutaneously generates electric power. The amount of reforming agents including CO_2 and oxygen ions (controlled by discharge current) is provided according to the stoichiometric amount of methane. Thereby, the new concept of electrochemical autothermal reforming of methane can be realized.

Another strategy to deal with methane-fueled SOFCs is applying reforming catalysts on anode side to improve reforming performance [23, 26]. The catalysts are either coated on anode surface or deposited on porous anode frame surface [27]. Coating a powder catalyst layer over anode surface enables the pre-reforming of methane before entering into porous anode layer. However, the porous catalyst layer induces gas diffusion limitation and current collection issue due to its poor electronic conductivity. The current collection issue can be eliminated by depositing nanocatalysts within porous anodes through an impregnation process. As anode-supported SOFCs are widely used, catalyst precursors readily accumulate near anode surface instead of reaching the interface between anode and electrolyte [28], where carbon deposition

greatly affects cell performance. In addition, the catalyst accumulation may cause gas blockage [29, 30]. Our previous study has reported fibrous catalyst beds packed within the channels of anode support of SOFC show the high catalytic performance of methane reforming [27].

In this study, the SOFC reformer was employed to demonstrate the new concept of the electrochemical autothermal reforming of methane for syngas production as well as power generation. Moreover, the exothermal fuel oxidation and endothermal DRM can be effectively coupled to realize autothermal reforming. The contribution of the catalyst bed reformer to the autothermal reforming was investigated by comparison with conventional SOFC reactors.

2. Experimental

2.1. SOFC preparation

SOFC reactors were prepared using the processes reported in our previous study [27]. All ceramic powders were purchased from Fuelcell Materials in USA. Firstly, NiO-$Y_{0.16}Zr_{0.84}O_{1.92}$(YSZ) anode supports were prepared by a mesh-assisted phase-inversion process. Polyethersulfone (PESF, Radel-A300) was gradually dissolved in N-methyl-2-pyrrolidone (NMP, 99%, Shanghai McLean Biochemical Co., Ltd., China) by magnetic stirring to form a 15 wt% PESF/NMP solution. Then, 36.99 g of NiO (NiO-F) and 24.66 g of YSZ (YSZ-TC) were dispersed in 28.32 g of the above solution by ball-milling for 48 h in a planetary ball-miller (Kejing, China) with adding 0.432 g of polyvinylpyrrolidone (PVP, MW = 40,000, Shanghai Dibo Biotechnology Co., Ltd., China) as a dispersant. Phase-inversion process was conducted in a mold assembled

with mesh by applying water on the tope of slurry as a coagulant. After 1.5 h, anode support green body was obtained after de-moulding, followed by drying in an oven set at 55 °C overnight. To prepare SOFCs, anode support was pre-sintered at 1050 °C for 2 hours. A YSZ-$Gd_{0.1}Ce_{0.9}O_2$ (GDC) electrolyte dual-layer was prepared by subsequently dip-coating and sintering to ensure high open circuit voltage (OCV) and prevent solid reaction between YSZ and perovskite cathode. YSZ (YSZ-U1) and GDC (GDC-TC) powders were dispersed in ethanol by ball-milling for 24 h to obtain uniformly electrolyte slurry, respectively. YSZ slurry and GDC slurry were dip-coated subsequently on anode skin layer surface. After co-sintering at 1350 °C for 5 h, an electrolyte layer was formed. Finally, a cathode layer of $La_{0.6}Sr_{0.4}Co_{0.8}Fe_{0.2}O_3$ (LSCF)-GDC was prepared by a spraying coating. 70 wt% of LSCF and 30 wt% of GDC were dispersed in ethanol by ball-milling for 24 hours to obtain a slurry with a solid content of 10 wt%. It was deposited on the electrolyte by spray-coating and sintering at 1050 °C for 2 h to form LSCF/GDC cathode layer. The active area of the cathode is about 0.6 cm^2.

2.2 Catalyst preparation

To improve anode catalytic activity, CeO_2 nanoparticle colloid (CeO_2 (AC), Naycol Nano Technology, Inc.) was infiltrated within anode support through microchannels [31]. After drying at 70 °C and sintering at 750 °C, a nanocatalyst layer is formed. Nanofibrous Ni/CeO_2-Al_2O_3 catalyst was prepared by an electrospinning process [32, 33]. 0.43 g of $Ni(NO_3)_2 \cdot 6H_2O$, 0.20 g of $Ce(NO_3)_3 \cdot 6H_2O$, 1.08 g of $Al(NO_3)_3 \cdot 9H_2O$,

1.00 g of PVP, 8.00 g of H_2O and 2.00 g of ethanol were mixed to form uniform solution under magnetic stirring. The prepared solution was spun into fibrous catalyst precursor through an electrospinning device (Beijing Yongkang Liye Technology Co., Ltd.), and catalyst precursor was sintered at 800 °C for 4 h to form a nanofibrous catalyst. The catalyst was ground in a mortar jar into ceramic fibres with a length less than 10 μm and then ultrasonically dispersed in ethanol (Fig. S1). The catalyst dispersion was drop-filled into channels with the assistance of vacuum and drying, and the process was repeated to achieve the loading amount of about 6.5 mg, which is controlled by cell weigh gains. A porous CuO (45.1 wt%)-GDC layer was coated over the outer surface of anode support to seal the fibrous catalysts within channels. For comparison, the fibrous catalyst was also coated on anode surface [27].

2.3 Characterization and testing of SOFC reformers

NiO/YSZ anode was reduced by hydrogen, and then feeding gas was switched to CH_4/CO_2/Ar mixture. CH_4 concentration was set as 25% while CO_2 concentration was tuned according to discharge current to ensure the total stoichiometric amount of reforming agents (CO_2 and O^{2-}) equal to methane. Cell performance and anode effluent gas composition were tested at different CH_4/CO_2 ratios, current densities and temperatures. An electrochemical workstation (Reference 3000, Gamry) was used to test cell performance. Anode gas was analyzed using a gas chromatograph (Shimadzu GC-2014). Scanning electron microscope (SEM, Zeiss Neon 40EsB FIBSEM) was used to observe cell microstructure.

2.4 Model development

A computational simulation platform (COMSOL V5.2) was used to simulate the 2D concentration distribution of species in one exemplary channel of SOFC reactors with and without catalysts embedded by finite element method (Modelling Methods, Supporting Information) at a current density of 1.05 A cm^{-2} [2]. Other operation conditions for the modelled were set to be the same as experimental conditions.

3 Results and discussion

3.1 SOFC autothermal reformer

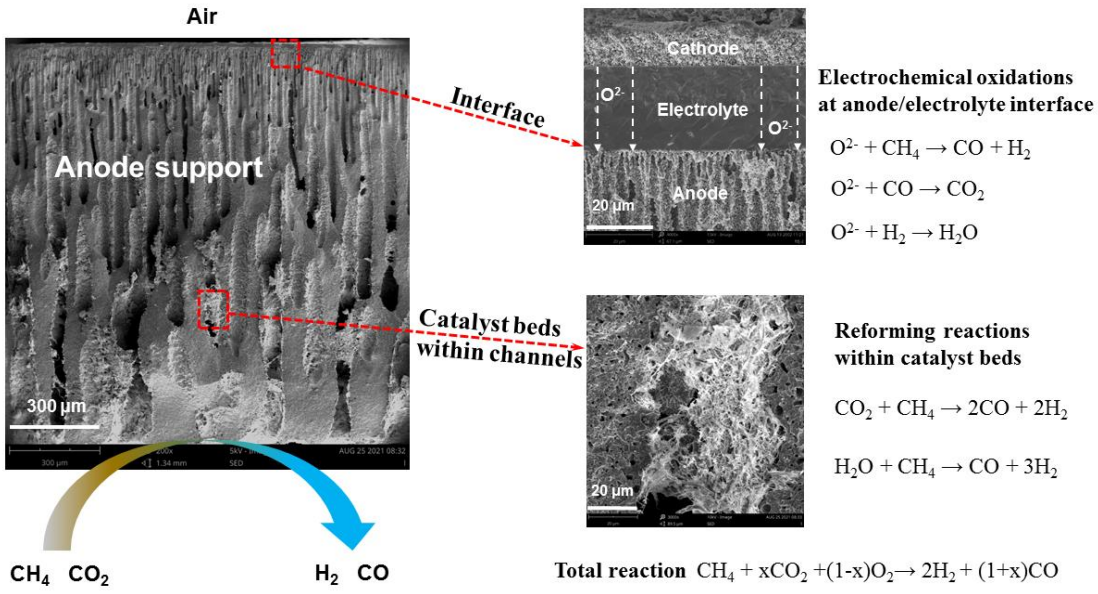

Fig. 2. Electrochemical autothermal reforming of methane over SOFC reactor integrated with catalyst bed reformer. The SEM images show catalyst bed location within channels and cell sandwich structure after test.

SOFCs with channeled anode supports were employed to perform the electrochemical autothermal reforming of methane. As shown in Fig. 2, anode support

has dendritic channel structure, with porosity of about 47.8% and channel size gradually decreasing from 80-100 μm on anode surface to 1-2 μm at the interface between anode support and electrolyte (Fig. S2) [27], which enables building catalyst bed micro-reformer. Nanofibrous Ni/CeO_2-Al_2O_3 catalyst was loaded into channels to form catalyst beds for conducting methane reforming. Catalyst beds mainly located near anode support surface during the test due to cell position and gas diffusion flow. Methane and CO_2 are fed on anode side; oxygen on cathode side exposed to air is reduced and the formed oxygen ions are transferred to anode side through electrolyte. Methane is reformed either directly by CO_2 over catalyst beds or indirectly by oxygen ions at the interface, as called electrochemical autothermal reforming of methane. Since syngas (CO and H_2) generated by methane reforming is more reactive than methane for electrochemical oxidation, syngas can diffuse to the interface and is then oxidized by oxygen ions. The oxidation products of steam and CO_2 react with methane over the catalyst beds to generate syngas. Accordingly, methane is likely reformed by oxygen ions indirectly. The total reaction is electrochemical autothermal reforming of methane.

3.2 Reforming and power generation performance

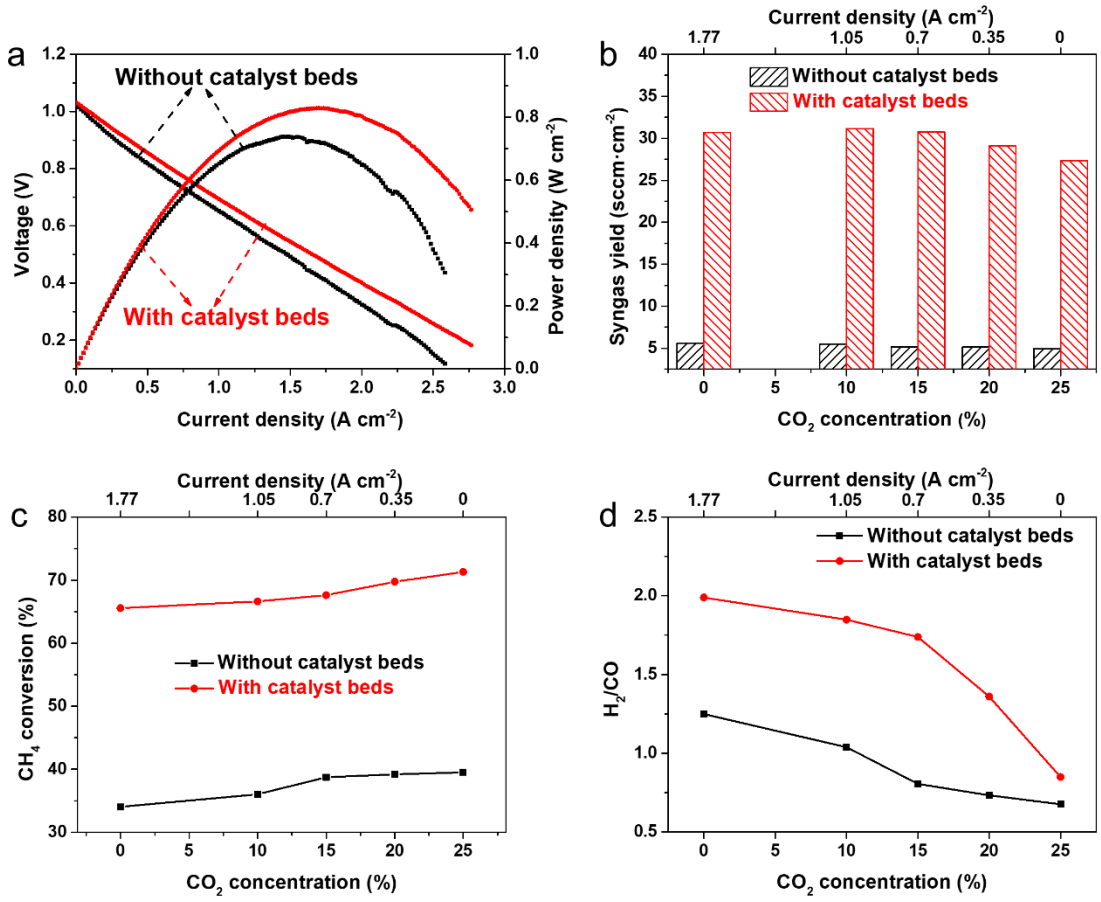

Fig. 3. Power generation and methane reforming performance at 800 °C over SOFC with and without catalyst bed reformer with a feeding of 25%CH_4/x CO_2/Ar mixture: (a) Power generation; (b) Syngas yield; (c) Methane conversion; (d) H_2/CO ratio.

The electrochemical autothermal reforming of methane was conducted over the SOFC integrated with catalyst bed reformer as well as the SOFC without catalyst beds for comparison. As shown in Fig. 3, the SOFC with catalyst beds generated the higher peak power density of 0.83 W cm^{-2} than that (0.74 W cm^{-2}) of the SOFC without catalyst beds when a gas mixture of 25%CH_4/25% CO_2/Ar was fed into the cells. It is attributed to the lower electrode polarization resistance of the SOFC with catalyst beds (Fig. S3), which is because that more syngas was formed over the catalyst beds and presented at the anode/electrode interface for electrochemical oxidation and syngas is more active

than methane.

Syngas generation through the electrochemical autothermal reforming was investigated at the different CO_2/O^{2-} ratios *via* gradually replacing current with CO_2, and the total stoichiometric amount of CO_2 and O^{2-} was retained the same as methane amount to realize autothermal reforming. The discharge current is calculated according to the corresponding O^{2-} amount. The SOFC with catalyst beds generated a much higher syngas yield (above 6 times) than that of the SOFC without catalyst beds. For example, at the current density of 1.05 A cm^{-2} and CO_2 concentration of 10%, syngas yields are 5.49 and 31.16 sccm·cm^{-2}, respectively. The higher syngas yields are attributed to the catalyst bed reformer, which doubles methane conversion and increases H_2 selectivity by a factor of above 3 (Fig. 3c and Fig. S4). As the discharge current was gradually replaced by CO_2 as a reforming agent, methane conversion was increased, which is attributed to the different flow directions of CO_2 and O^{2-} with methane (concurrent flow *vs.* counter flow). Moreover, the SOFC with catalyst beds generates syngas with a large range of H_2/CO ratio (0.81-2.00) by tuning CO_2/O^{2-} ratio. In contrast, the H_2/CO ratio by the SOFC without catalyst beds is limited in a small range of 0.72-1.25. Therefore, the catalyst bed reformer ensured the high performance of the electrochemical autothermal reforming.

3.3 Effect of integrated reformer

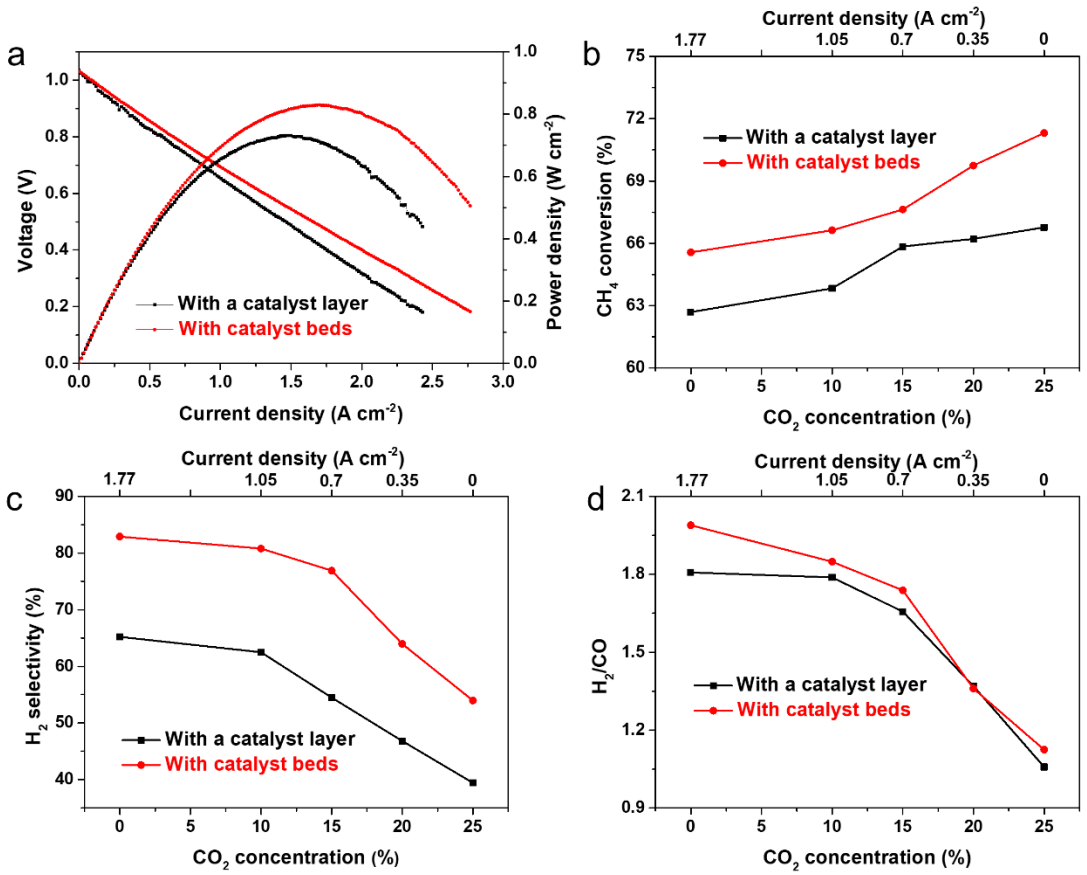

Fig. 4. Power generation and autothermal reforming performance at 800 °C over SOFCs with a catalyst layer on anode surface and catalyst beds within anode channels: (a) Power density; (b) Methane conversion; (c) H_2 selectivity; (d) H_2/CO ratio.

To confirm the efficient reforming over the catalyst beds, Ni/CeO_2-Al_2O_3 fibrous catalyst was also coated on anode surface as conventional anode catalyst layer for comparison. 29.1 mg of Ni/CeO_2-Al_2O_3 catalyst was deposited on anode surface to form a catalyst layer with a thickness of 30-40 μm while only 6.5 mg of the fibrous catalyst was used to pack the catalyst beds within channels (Fig. S5). The catalyst beds generated the higher methane conversion and syngas selectivity in methane reforming than the catalyst layer in Fig. 4, indicating the higher reforming performance of catalyst

beds within channels. It might be because the gases have the longer contact time with catalyst beds when diffusing through anode supports. In addition, as the less CO_2 was used, the SOFC with catalyst beds generated syngas with the higher H_2/CO ratio than the SOFC with a catalyst layer (Fig. 4d), which is close to 2 when the partial oxidation of methane by the SOFC was conducted. The higher reforming performance by the catalyst beds resulted in the higher power output. Therefore, the catalyst beds within anode support are more efficient than the catalyst layer on anode surface in the electrochemical autothermal reforming.

3.4 Temperature effect

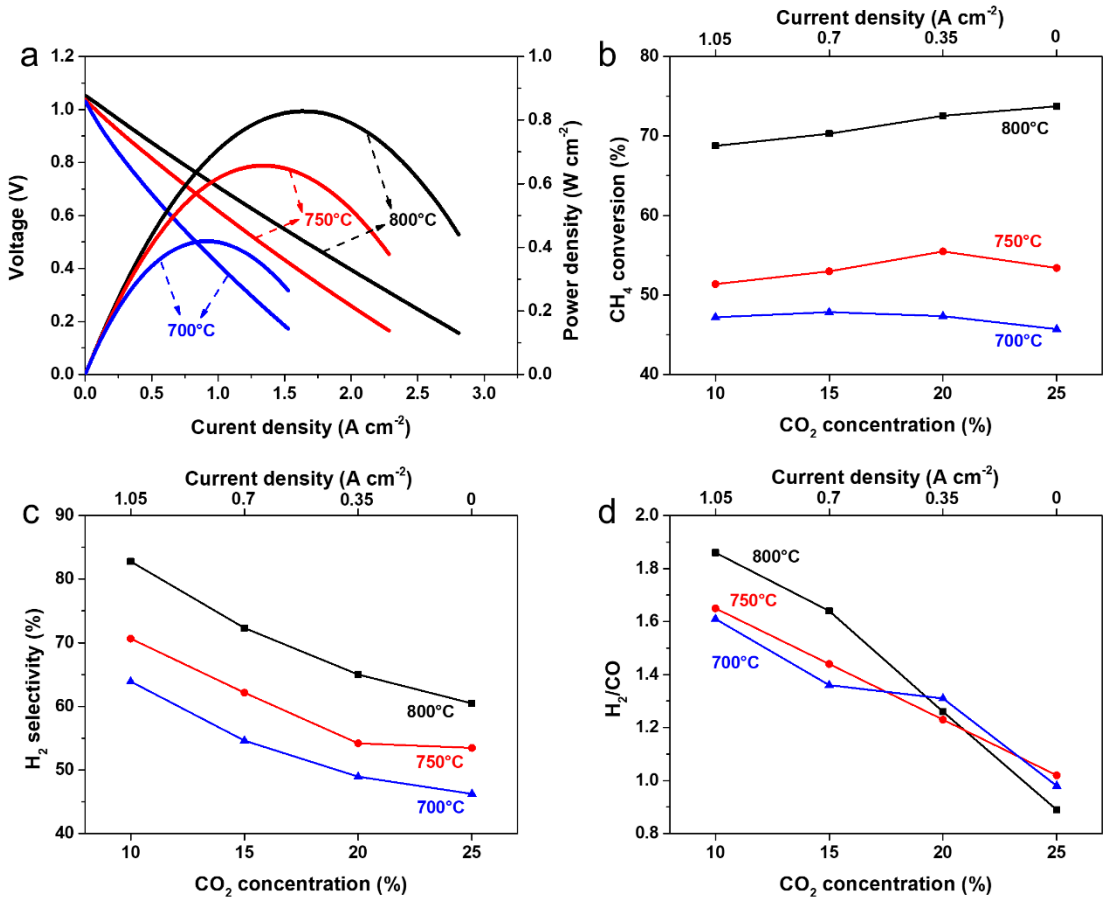

Fig. 5. Effect of operation temperature on power generation and methane reforming at 800 °C: (a) Power density; (b) Methane conversion; (c) H_2 selectivity; (d) H_2/CO ratio.

Since the autothermal reforming includes exothermal fuel oxidation and endothermal dry reforming, operation temperature would affect both power generation and methane reforming. As operation temperature was increased from 700 to 800 °C in Fig. 5, the maximum power density of the SOFC gradually increased from 0.42 to 0.83 W cm^{-2} owing to the decreased cell resistance (Fig. S6). In addition, methane conversion and H_2 selectivity increased with operation temperature because of the increased catalytic activity of the reforming catalysts. Operation temperature also influences the effect of CO_2/O^{2-} ratio on methane conversion. Methane conversion increases with the CO_2/O^{2-} ratio at 800 °C as discussed above, while it gradually becomes decreasing as operation temperature is decreased. It is because operation temperature has the larger influence on extensive endothermal dry reforming than weak exothermal methane partial oxidation. The H_2/CO ratios of methane dry reforming are close to 1.0 at all operation temperatures, and they are increased with decreasing CO_2/O^{2-} ratio because methane partial oxidation plays more roles. Methane reforming at high operation temperatures generates more hydrogen for electrochemical oxidation than that at low temperatures, resulting in high H_2/CO ratios.

To compare the methane reforming performance with conventional catalyst bed reactors, the fibrous Ni/CeO_2-Al_2O_3 catalyst was packed in a quartz reactor to test autothermal reforming of methane [32]. Although a larger amount (38.6 mg) of catalyst was packed in the reactor to form uniform bed, the reactant gases/catalyst ratio was retained the same as that in the SOFC reactor. The fixed-bed reactor was tested under

autothermal reforming and dry reforming with the feeding gases of 25%CH_4/10%CO_2/7.5%O_2/Ar and 25%CH_4/25%CO_2/Ar, respectively. Compared with the SOFC reformer, the conventional fixed-bed reactor generated the similar methane conversion of ~70% at 800 °C and the higher methane conversion at 750 and 700 °C (Fig. S7), which might be related to more efficient thermal coupling effect. The conventional fixed-bed reactor has efficient mass transfer by one-path flow through catalyst bed while the mass transfer of the SOFC reformer mainly relies on gas diffusion. Accordingly, SOFCs not only generates power, but also contributes methane reforming through the catalytic activity of Ni-based anode. The conventional fixed-bed reactor generated the lower hydrogen selectivity (especially during autothermal reforming) and H_2/CO ratios (0.6-1.6) than the SOFC reformer. Therefore, the SOFC reformer generated comparable reforming performance as conventional fixed-bed reactors while generating electric power and eliminating the need of expensive oxygen.

3.5 Stability

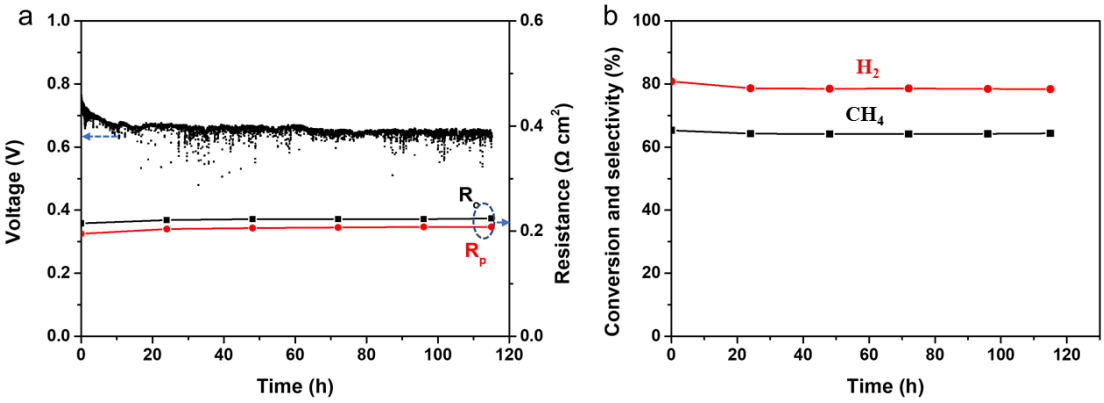

Fig. 6. Stability performance of electrochemical autothermal reforming at 800 °C over the SOFC integrated with catalyst bed reformer at a current density of 1.05 A cm^{-2} with a feeding gas of 25%CH_4/10%CO_2/Ar: (a) Applied potential, cell ohmic

resistance (R_o) and polarization resistance (R_p); (b) Methane conversion and H_2 selectivity.

The stability of the autothermal reforming was investigate at 800 °C and a discharge current density of 1.05 A cm^{-2} with a feeding gas of 25%CH_4/10%CO_2/Ar. As shown in Fig. 6, the cell voltage decreased within the initial 20 h, and then became stable during the test for 120 h. The initial decrease is attributed to the increased ohmic resistance (R_o) and polarization resistance (R_p), which might be caused by the stabilization of cell microstructure, such as catalyst and Ni activation [34]. During the test, methane conversion and syngas selectivity remained stable, indicating the stable reforming catalyst.

3.6 Numerical assessment of enhanced mass transportation

To probe the advantages of internal reforming in term of mass transfer, i.e. the *in-situ* coupled chemical reaction and optimized fuel specie distribution, the modelling of chemical and mass transfer in the integrated SOFC reformer was conducted and its counterpart with no catalyst beds (from the anode surface to the electrolyte, schemed by Fig. 7a).

As shown in Fig. 8b, methane reforming is significantly enhanced after integrating the catalyst bed. The consumption of CO_2 is also greatly reduced when species approach the electrolyte-electrode interface (E-E interface). As a result, the H_2 concentration profile is lifted. It should be noted that the CO concentration are the most enhanced, this is because the H_2 electrochemical oxidation at the E-E interface is assumed to be the dominating reaction over the CO electrochemical oxidation in the model. Looking

at the interplay of channel and wall in enhancing the mass transportation, the species flux of CH_4, CO_2 and H_2 are marked by arrows in Fig. 7c-e. The magnitude of flux is represented by the size of arrow. It can be observed the existence of channels serves as a highway for H_2 and H_2O product diffusion (see the black and cyan-colored arrows near the E-E interface). This clearly proves the internal integrated catalyst bed can facilitate the mass transportation due to the shortened diffusion pathway.

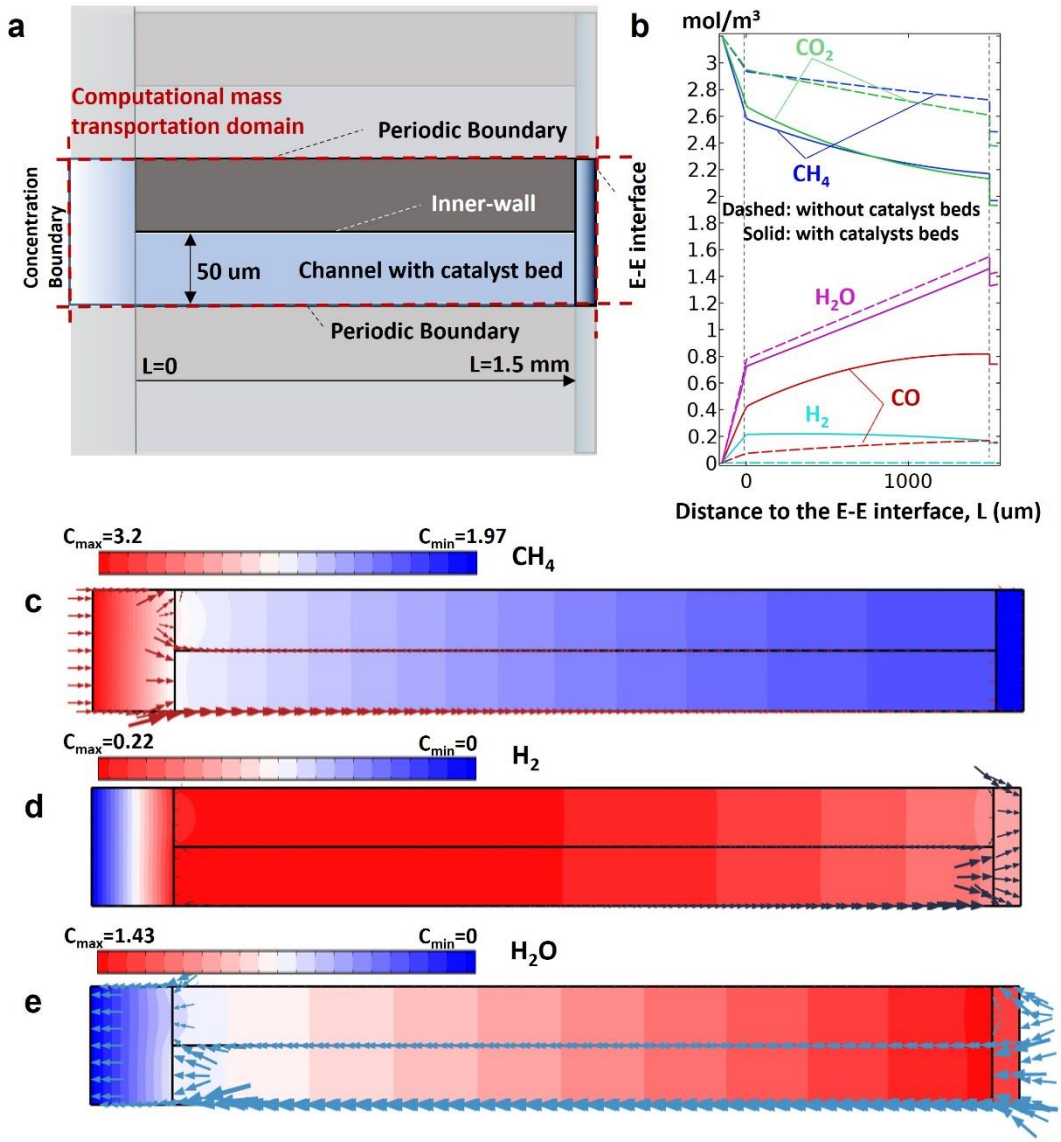

Fig. 7. Numerical modeling results of the integrated SOFC reformer with catalyst beds

embedded (not to scale): (a) Schematic of the computational domain with boundary marked; (b) Comparison of species concentration from anode surface to electrode-electrolyte interface along the inner wall; (c-e) Contours of species concentration (unit: mol/m^3) with its total flux marked with arrows for the integrated SOFC reformer.

To better evaluate the effectiveness of integrated catalyst bed design in mass transportation, we defined a characteristic fuel accessibility factor (χ) for the anode by quantify the easiness of transporting reformed products (taking H_2 as the tracing species) to reach the anode/electrolyte interface. The χ factor is developed from the classis Thiele modulus (φ) as shown by **Eq. 2** [35], which is defined by the ratio of reaction to the diffusion rate. The k is the first order reaction constant of individual reaction, L is the characteristic length and D_{eff} is the effective diffusion coefficient. Since the kinetic model used for reforming reactions is not first order, we modified the Thiele modulus expression to be as **Eq. 3**, using the total local generation rates of H_2 (R_{H_2}) to replace the first order reaction constant k. In addition, we apply the integral of modified Thiele modulus to fully assess the whole electrode in fuel generation and delivering, defined by the integral of the distance to anode/electrolyte interface, species fraction, the divided by diffusion coefficient.

$$\varphi = \sqrt{\frac{rate\ of\ reaction}{rate\ of\ diffsuion}} = \sqrt{kL^2/D_{eff}} \tag{2}$$

$$\chi = \iint_S R_{H_2} L^2/D_{eff}\ ds \tag{3}$$

Based on the simulation, the χ for integrated SOFC reactor is calculated as ca. 84.33, higher than that of the counterpart without catalyst (~64.30). Since this factor can be

used as the criteria for evaluating the fuel accessibility in case of combined catalytic reaction and mass transportation in porous medium, it can therefore verify that better fuel availability is achieved at the key anode/electrolyte interface of the integrated SOFC reformer, where majority of the electrochemical reaction occurs, and thus the concentration polarization is reduced. This is in good agreement with the enhanced power density in the experimental results of Fig. 4a, indicating the effectiveness of the unique anode structure not only in optimizing the reforming and enhancing, but also in enhancing the mass transportation.

4. Conclusions

This study has creatively employed the integrated SOFC reactor to perform the autothermal reforming of methane, and the electrochemical autothermal reformer eliminates the need of expensive oxygen and safety issue caused by CH_4/O_2 mixture in conventional autothermal reforming and generates electric power simultaneously. Catalyst bed reformer was integrated into channeled anode support to ensure the efficient methane reforming. Compared with the SOFC without the catalyst beds, the integrated SOFC increased syngas yield by a factor of about 6 times owing to the increased methane conversion and syngas yield by the catalyst beds. By simulation, this enhancement is successfully validated by a new proposed fuel accessibility factor as 86.9 (integrated SOFC reactor with catalyst beds) *vs.* 68.2 (that without catalyst beds). Compared with conventional catalyst layer on anode surface, the catalyst beds within anode channels are more efficient in methane reforming, resulting in higher syngas

yields and cell performance. The SOFC reformer demonstrated the stable autothermal reforming performance during the test for 120 h. Therefore, the integrated SOFC reformer is promising for conducting methane reforming with additional benefits.

Acknowledgements

Prof. Dong acknowledges financial supports from National Natural Science Foundation of China (51872123), Natural Science Foundation of Shandong Province (ZR2017MEM022) and Bureau of Science and Technology of Jinan (2020GXRC033). Dr. Chen would like to thank National Natural Science Foundation of China (No. 52006150) and Natural Science Foundation of Guangdong Province (No. 2020A1515010550) for support.

References

[1] H.S. Kim, Y. Jeon, J.H. Kim, G.Y. Jang, S.P. Yoon, J.W. Yun,Characteristics of Sr1−xYxTi1−yRuyO3+/−δ and Ru-impregnated Sr1−xYxTiO3+/−δ perovskite catalysts as SOFC anode for methane dry reforming, Applied Surface Science, 510 (2020) 145450.

[2] B. Chen, H. Xu, L. Chen, Y. Li, C. Xia, M. Ni,Modelling of One-Step Methanation Process Combining SOECs and Fischer-Tropsch-like Reactor, Journal of The Electrochemical Society, 163 (2016) F3001-F3008.

[3] Z. Shao, C. Zhang, W. Wang, C. Su, W. Zhou, Z. Zhu, H.J. Park, C. Kwak,Electric power and synthesis gas co-generation from methane with zero waste gas emission, Angewandte Chemie, 50 (2011) 1792-1797.

[4] Z. Lyu, W. Shi, M. Han,Electrochemical characteristics and carbon tolerance of solid oxide fuel cells with direct internal dry reforming of methane, Applied Energy, 228 (2018) 556-567.

[5] L. Barelli, G. Bidini, A. Di Michele, L. Gammaitoni, M. Mattarelli, F. Mondi, E. Sisani,Development and validation of a Ni-based catalyst for carbon dioxide dry reforming of methane process coupled to solid oxide fuel cells, International Journal of Hydrogen Energy, 44 (2019) 16582-16593.

[6] T. Zhu, Z. Yang, M. Han,Performance evaluation of solid oxide fuel cell with in-situ methane reforming, Fuel, 161 (2015) 168-173.

[7] G. Deng, G. Zhang, X. Zhu, Q. Guo, X. Liao, X. Chen, K. Li,Optimized Ni-based catalysts for methane reforming with O2-containing CO2, Applied Catalysis B: Environmental, 289 (2021) 120033.

[8] Y. Ma, Y. Ma, Y. Chen, S. Ma, Q. Li, X. Hu, Z. Wang, C.E. Buckley, D. Dong,Highly stable nanofibrous La2NiZrO6 catalysts for fast methane partial oxidation, Fuel, 265 (2020) 116861.

[9] G. Pauletto, N. Libretto, D.C. Boffito, J.T. Miller, A. Jentys, G.S. Patience, J.A. Lercher,Ni/CeO2 promoted Ru and Pt supported on FeCrAl gauze for cycling methane catalytic partial oxidation—CPOX, Applied Catalysis B: Environmental, 286 (2021) 119849.

[10] D. Pashchenko, I. Makarov,Carbon deposition in steam methane reforming over a Ni-based catalyst: Experimental and thermodynamic analysis, Energy, 222 (2021) 119993.

[11] J. Martin-del-Campo, M. Uceda, S. Coulombe, J. Kopyscinski,Plasma-catalytic dry reforming of methane over Ni-supported catalysts in a rotating gliding arc – Spouted bed reactor, Journal of CO2 Utilization, 46 (2021) 101474.

[12] B. Chen, H. Xu, Y. Zhang, F. Dong, P. Tan, T. Zhao, M. Ni,Combined methane reforming

by carbon dioxide and steam in proton conducting solid oxide fuel cells for syngas/power co-generation, International Journal of Hydrogen Energy, 44 (2019) 15313-15321.

[13] R. Carapellucci, L. Giordano,Steam, dry and autothermal methane reforming for hydrogen production: A thermodynamic equilibrium analysis, Journal of Power Sources, 469 (2020) 228391.

[14] J. Chen, J. Han, D. Xu,Efficient operation of autothermal microchannel reactors for the production of hydrogen by steam methane reforming, International Journal of Hydrogen Energy, 44 (2019) 11546-11563.

[15] N. Lu, F. Gallucci, T. Melchiori, D. Xie, M. Van Sint Annaland,Modeling of autothermal reforming of methane in a fluidized bed reactor with perovskite membranes, Chemical Engineering and Processing - Process Intensification, 124 (2018) 308-318.

[16] H.-x. You, H.-j. Gao, G. Chen, A. Abulit, X.-w. Ding,Reactions of low concentration dry methane at Ni-YSZ anode in the SOFCs, Journal of Fuel Chemistry and Technology, 39 (2011) 69-74.

[17] V.N. Nguyen, R. Deja, R. Peters, L. Blum,Methane/steam global reforming kinetics over the Ni/YSZ of planar pre-reformers for SOFC systems, Chemical Engineering Journal, 292 (2016) 113-122.

[18] A. Lanzini, P. Leone, C. Guerra, F. Smeacetto, N.P. Brandon, M. Santarelli,Durability of anode supported Solid Oxides Fuel Cells (SOFC) under direct dry-reforming of methane, Chemical Engineering Journal, 220 (2013) 254-263.

[19] Z. Lyu, H. Li, M. Han,Electrochemical properties and thermal neutral state of solid oxide fuel cells with direct internal reforming of methane, International Journal of Hydrogen Energy,

44 (2019) 12151-12162.

[20] D. Lee, J. Myung, J. Tan, S.-H. Hyun, J.T.S. Irvine, J. Kim, J. Moon,Direct methane solid oxide fuel cells based on catalytic partial oxidation enabling complete coking tolerance of Ni-based anodes, Journal of Power Sources, 345 (2017) 30-40.

[21] A. Ideris, E. Croiset, M. Pritzker, A. Amin,Direct-methane solid oxide fuel cell (SOFC) with Ni-SDC anode-supported cell, International Journal of Hydrogen Energy, 42 (2017) 23118-23129.

[22] K. Girona, J. Laurencin, J. Fouletier, F. Lefebvre-Joud,Carbon deposition in CH4/CO2 operated SOFC: Simulation and experimentation studies, Journal of Power Sources, 210 (2012) 381-391.

[23] W. Wang, R. Ran, C. Su, Z. Shao, D.W. Jung, S. Seo, S.M. Lee,Effect of nickel content and preparation method on the performance of Ni-Al2O3 towards the applications in solid oxide fuel cells, International Journal of Hydrogen Energy, 36 (2011) 10958-10967.

[24] L. Barelli, G. Bidini, G. Cinti, F. Gallorini, M. Pöniz,SOFC stack coupled with dry reforming, Applied Energy, 192 (2017) 498-507.

[25] D.H. Prasad, S.Y. Park, H. Ji, H.R. Kim, J.W. Son, B.K. Kim, H.W. Lee, J.H. Lee,Effect of steam content on nickel nano-particle sintering and methane reforming activity of Ni–CZO anode cermets for internal reforming SOFCs, Applied Catalysis A: General, 411-412 (2012) 160-169.

[26] Y. Akdeniz, B. Timurkutluk, C. Timurkutluk,Development of anodes for direct oxidation of methane fuel in solid oxide fuel cells, International Journal of Hydrogen Energy, 41 (2016) 10021-10029.

[27] D. Fan, F. Liu, J. Li, T. Wei, Z. Ye, Z. Wang, X. Hu, D. Dong, H. Wang, Z. Shao,A microchannel reactor-integrated ceramic fuel cell with dual-coupling effect for efficient power and syngas co-generation from methane, Applied Catalysis B: Environmental, 297 (2021) 120443.

[28] P. Keyvanfar, V. Birss,Optimization of Infiltration Techniques Used to Construct Ni/YSZ Anodes, Journal of the Electrochemical Society, 161 (2014) F660-F667.

[29] B.J.M. Sarruf, J.-E. Hong, R. Steinberger-Wilckens, P.E.V. de Miranda,CeO2Co3O4CuO anode for direct utilisation of methane or ethanol in solid oxide fuel cells, International Journal of Hydrogen Energy, 43 (2018) 6340-6351.

[30] B. Han, K. Zhao, X. Hou, D.-J. Kim, B.-H. Kim, S. Ha, M.G. Norton, Q. Xu, B.-G. Ahn,Ni-(Ce0.8-xTix)Sm0.2O2-δ anode for low temperature solid oxide fuel cells running on dry methane fuel, Journal of Power Sources, 338 (2017) 1-8.

[31] J. Wang, T. Wang, L. Yu, T. Wei, X. Hu, Z. Ye, Z. Wang, C.E. Buckley, J. Yao, G.E. Marnellos, D. Dong,Catalytic CeO2 washcoat over microchanneled supporting cathodes of solid oxide electrolysis cells for efficient and stable CO2 reduction, Journal of Power Sources, 412 (2019) 344-349.

[32] Y. Ma, Y. Ma, Z. Zhao, X. Hu, Z. Ye, J. Yao, C.E. Buckley, D. Dong,Comparison of fibrous catalysts and monolithic catalysts for catalytic methane partial oxidation, Renewable Energy, 138 (2019) 1010-1017.

[33] Y.X. Ma, Y.Y. Ma, J.J. Li, Q.G. Li, X. Hu, Z.M. Ye, X.Y. Wu, C.E. Buckley, D.H. Dong,CeO2-promotion of NiAl2O4 reduction via CeAlO3 formation for efficient methane reforming, J. Energy Inst., 93 (2020) 991-999.

[34] A. Hauch, S.H. Jensen, S. Ramousse, M. Mogensen,Performance and durability of solid oxide electrolysis cells, Journal of the Electrochemical Society, 153 (2006) A1741-A1747.

[35] I. Tosun, Modeling in transport phenomena: a conceptual approach, Elsevier, 2007.